Synthesis of Hybrid Organo−Mineral Materials: Anionic Tetraphenylporphyrins in Layered Double Hydroxides

S. Bonnet, C. Forano, A. de Roy, and J. P. Besse*

Laboratoire de Physico-Chimie des Matériaux, CNRS URA 444, Université Blaise-Pascal, 63177 Aubière Cedex, France

P. Maillard and M. Momenteau

Institut Curie, Section de Biologie, CNRS URA 1387, Bât 112, Centre Universitaire, 91405 Orsay, France

Received January 11, 1996. Revised Manuscript Received May 1, 1996[⊗]

meso-Tetrakis(*p*-carboxyphenyl)porphyrin (*p*TCPP), the atropoisomer (αααα) of *meso*-tetrakis(*o*-carboxyphenyl)porphyrin (*o*TCPP), and the ammonium salt of the *meso*-tetrakis-(*p*-sulfonatophenyl)porphyrin (noted *p*TSPP) were intercalated into [Zn−Al] layered double hydroxide (LDH) using different preparative methods. Coprecipitation at constant pH in a porphyrinic solution of zinc and aluminum salts or anionic exchange of *p*TCPP on a [Zn−Al−Cl] precursor led to pure LDH phases, while products obtained from the calcination−reconstruction method on a [Zn−Al−Cl] precursor contain a significant amount of ZnO. Powder X-ray diffraction and UV−visible diffuse reflectance spectroscopy of LDH intercalated with *p*TCPP, *o*TCPP, and *p*TSPP show complete intercalation. Interlayer spacing ranging from 18.54 Å for [Zn−Al−*o*TCPP] to 22.91 Å for [Zn−Al−*p*TSPP] and 22.73 Å for [Zn−Al−*p*TCPP], determined from PXRD patterns, reveal different orientations of the anionic macrocyles between the hyroxylated layers. This selective arrangement is discussed in terms of layer charge density, isomeric substitution of the anionic groups on the *meso* tetraphenylporphyrins, and guest molecules and host matrix interactions.

Introduction

Recently, there has been much interest in the immobilization of porphyrins, phthalocyanines and their metallo derivatives on inorganic supports. A large number of mineral structures including layered double hydroxides,[1−7] clays,[2,3,8−14] zeolites,[15,16] layered phosphates and phosphonates,[17,18] and silica and alumina[19−21] have been involved.

Such new nanocomposite hybrid materials have shown interesting properties in heterogeneous catalysis for alkane hydroxylation, alkene epoxidation,[1,2,8,16,20,22] alcohol and hydrocarbon oxidation,[16,23,24] and activation of molecular species such as nitrous ions.[25] These materials have also been used as photochemical hole-burning materials[25,26] and could find interesting applications as electrochemical microsensors in the form of clay-modified electrodes[27,28] or as gas or optical sensors.

Most of these novel materials concern metalloporphyrins and mainly *meso*-tetraphenylporphyrin molecules adsorbed in an ionic form on mineral supports: smectites (hectorite and montmorillonite), zeolites, and LDHs. These three inorganic host materials offer adsorption regions of different natures: zeolites behave as structurally constrained tridimensional systems while

* To whom all correspondence should be addressed.

[⊗] Abstract published in *Advance ACS Abstracts,* July 15, 1996.

(1) Park, I. Y.; Kuroda, K.; Kato, C. *Chem. Lett.* **1989**, 2057.
(2) Barloy, L.; Lallier, J. P.; Battioni, P.; Mansuy, D.; Piffard, Y.; Tournoux, M.; Valim, J. B.; Jones, W. *New J. Chem.* **1992**, *16*, 71.
(3) Ukrainczyk, L.; Chibwe, M.; Pinnavaia, T. J.; Boyd, S. A. *J. Phys. Chem.* **1994**, *98*, 2668.
(4) Perez-Bernal, M. E.; Ruano-Casero, R.; Pinnavaia, T. J. *Catal. Lett.* **1991**, *11*, 55.
(5) Chibwe, M.; Pinnavaia, T. J. *J. Chem. Soc., Chem. Commun.* **1993**, 278.
(6) Carrado, K. A.; Forman, J. E.; Botto, R. E.; Winans, R. E. *Chem. Mater.* **1993**, *5*, 472.
(7) Pinnavaia, T. J.; Chibwe, M.; Constantino, V. R. L.; Yun, S. K. *Appl. Clay Sci.* **1995**, *10*, 117.
(8) Barloy, L.; Battioni, P.; Mansuy, D. *J. Chem. Soc., Chem. Commun.* **1990**, 1365.
(9) Kosiur, D. R. *Clays Clay Miner.* **1977**, *25*, 365.
(10) Van Damme, H.; Crespin, M.; Obrecht, F.; Cruz, M. I.; Fripiat, J. J. *J. Colloid Interface Sci.* **1978**, *66*, 43.
(11) Cady, S. S.; Pinnavaia, T. J. *Inorg. Chem.* **1978**, *17*, 1501.
(12) Carrado, K. A.; Winans, R. E. *Chem. Mater.* **1990**, *2*, 328.
(13) Carrado, K. A.; Thiyagarajan, P.; Winans, R. E.; Botto, R. E. *Inorg. Chem.* **1991**, *30*, 794.
(14) Kameyama, H.; Suzuki, H.; Amano, A. *Chem. Lett.* **1988**, 1117.
(15) De Vismes, B.; Bedioui, F.; Devynck, J.; Bied-Charreton, C. *J. Electroanal. Chem.* **1985**, *187*, 197.
(16) De Vismes, B.; Bedioui, F.; Devynck, J.; Bied-Charreton, C.; Perrée-Fauvet, M. *Nouv. J. Chim.* **1986**, *10*, 81.
(17) Kim, R. M.; Pillion, J. E.; Burwell, D. A.; Groves, J. T.; Thompson, M. E. *Inorg. Chem.* **1993**, *32*, 4509.
(18) Deniaud, D.; Schöllorn, B.; Mansuy, D.; Rouxel, J.; Battioni, P.; Bujoli, B. *Chem. Mater.* **1995**, *7*, 995.
(19) Cooke, P. R.; Lindsay Smith, J. R. *J. Chem. Soc., Perkin Trans.* **1994**, 1913.
(20) Fukuzumi, S.; Mochizuki, S.; Tanaka, T. *Isr. J. Chem.* **1987/88**, *28*, 29.
(21) Battioni, P.; Lallier, J. P.; Barloy, L.; Mansuy, D. *J. Chem. Soc., Chem. Commun.* **1989**, 1149.
(22) Herron, N. *J. Coord. Chem.* **1988**, *19*, 25.
(23) Bedioui, F.; Gutierrez Granados, S.; Devynck, J. *New. J. Chem.* **1991**, *15*, 939.
(24) Herron, N.; Stucky, G. D.; Tolman, C. A. *J. Chem. Soc., Chem. Commun.* **1986**, 1521.
(25) Bedioui, F.; Bouhier, Y.; Sorel, C.; Devinck, J.; Coche-Guerente, L.; Deronzier, A.; Moutet, J. *Electrochim. Acta.* **1993**, *38*, 2485.
(26) Sakado, K.; Kominami, K.; Iwamoto, M. *Jpn. J. Appl. Phys.* **1988**, *27*, L1304.
(27) Mousty, C.; Therias, S.; Forano, C.; Besse, J. P. *J. Electroanal. Chem.* **1994**, *374*, 63.
(28) Therias, S.; Mousty, C. Special issue of Appl. Clay Sci. "Industrial Applications of Anionic Clays"; Vaccary, A., Ed.; Elsevier: Amsterdam, 1994.

S0897-4756(96)00020-8 CCC: $12.00

cationic and anionic clays display open-layered frameworks. Among the clays family, LDH are known to display higher expansion properties. These major structural differences can be used in novel ways for the design of new nanoreactors with different host−guest arrangements.

In catalyzed chemical processes, major advantages can be obtained by this association in terms of activity and selectivity. In their cationic or anionic forms the porphyrins and phthalocyanines display a very high affinity toward respectively negatively or positively charged inorganic supports. The charge density of the layers directly controls the concentration of the catalytic species. This can be quite high, especially with high charge density supports such as layered zirconium phosphates or layered double hydroxides (LDH). Indeed, LDH display very high ionic exchange capacities compared to the cationic-exchange capacity of the clay minerals. As an example, the calculated anion-exchange capacity (aec) of $Zn_3Al(OH)_8Cl{\cdot}nH_2O$ (abbreviated [Zn_3−Al−Cl]) is about 250 mequiv/100 g of dried LDH, much greater than the value for a hectorite-type cationic clay (80 mequiv/100 g).

A high regioselectivity can be expected from the structural arrangement of the guest−host system provided diffusion of reagents and products in the network is favored. The reactivity (acidity or basicity) of the mineral support can also combine to add a chemical selectivity to this stereospecificity.

Moreover, the guest−host interactions have shown in the case of porphyrins adsorbed on clays improved chemical stability, including the prevention of rapid photodegradation of the organic macrocycles.

We describe in this paper the incorporation of carboxylate and sulfonate porphyrins in [Zn−Al] LDH systems by various preparative methods. The porphyrin molecules are immobilized as the following anionic species: *meso*-tetrakis(*p*-carboxyphenyl)porphyrin (*p*TCPP), the atropoisomer (αααα) of *meso*-tetrakis-(*o*-carboxyphenyl)porphyrin (*o*TCPP), and the ammonium salt of the *meso*-tetrakis(*p*-sulfonatophenyl)-porphyrin (*p*TSPP). The structures of the porphyrins are presented in Figure 1. The structural arrangement of these various guest molecules in the LDH interlayers related to the isomeric nature of porphyrins and the charge density of the LDH layers is discussed. The results are also compared with the results of other mineral supports.

Experimental Section

Materials and Methods. *Porphyrins.* *p*TCPP, *o*TCPP, and *p*TSPP are synthesized according to a previously described method.[29−32]

The prepared LDH phases will be named according to the abbreviated nomenclature $[Zn_R-Al-X]_{prep}$, where R is the Zn^{2+}/Al^{3+} ratio of the metallic salt reagent solution used in coprecipitation method,[33,34] and X is the intercalated anion. The subscript prep stands for the preparation method: cop for coprecipitation at constant pH, exc for anionic exchange reaction, rec for calcination−reconstruction method, and hyd for hydrothermal treatment.

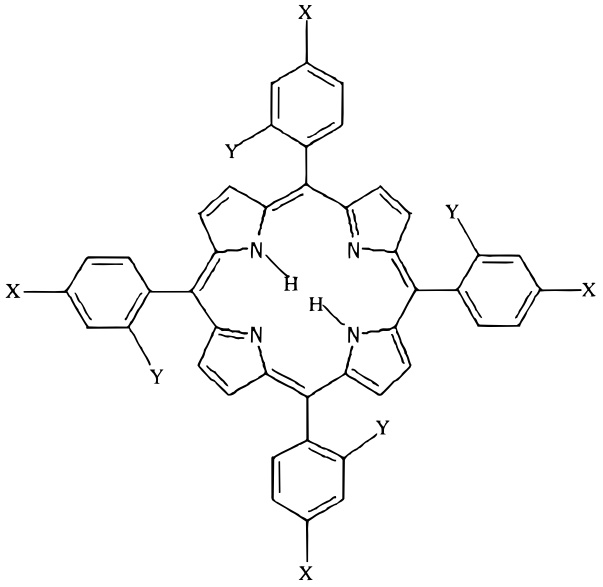

Figure 1. Structure of the porphyrins used in this study: *p*TCPP X = COOH, Y = H; *o*TCPP X = H, Y = COOH; *p*TSPP X = SO_3H, Y = H.

Table 1. Chemical Analyses of the Products

products	LDH layers Zn/Al	anionic species C/N	S/N	N/Al	Al/Cl
$[Zn_3-Al-Cl]_{cop}$	2.70				0.87
$[Zn_5-Al-Cl]_{cop}$	4.23				0.82
$[Zn_3-Al-pTCPP]_{exc}$	2.59	12.6		1.24	26
$[Zn_3-Al-pTCPP]_{cop}$	2.59	12.4		1.06	28
$[Zn_3-Al-pTSPP]_{cop}$	2.54	11.2	1.11	0.57	11
$[Zn_3-Al-pTSPP]_{hyd}$	2.54	12.0	0.89	0.59	13
$[Zn_3-Al-oTCPP]_{cop}$	2.45	13.6		1.18	23

$[Zn_3-Al-Cl]_{cop}$ is prepared by coprecipitation as follows: 40 mL of a zinc chloride (0.75 M) and aluminum chloride (0.25 M) solution is added at a rate of 0.603 mL min^{-1} in a flask containing 150 mL of distilled and deionized water, at room temperature, with vigorous stirring. A solution of sodium hydroxide (2 M) is simultaneously added. This addition is monitored via a pH electrode immersed in the reagent solution in order to fix the pH of coprecipitation at 7.0 ± 0.2. The addition of the metallic salt solution is completed in 1 h, and the mixture is then left to react for 2 days. The LDH is recovered by six dispersion and centrifugation cycles in deionized water, with a 3% mass ratio of solid in suspension. The gelatinous precipitate is finally air-dried. Chemical analysis confirms a typical composition of anionic clays with a ratio of Zn^{2+}/Al^{3+} equal to 2.70 (Table 1). A hydration state of 2.9 H_2O molecules/Al^{3+} cation was measured by TGA.

$[Zn_5-Al-Cl]_{cop}$ is prepared by using the same procedure as for $[Zn_3-Al-Cl]_{cop}$. Concentration of the metallic salt solution of zinc and aluminum chloride was, respectively, 0.8 and 0.16 M, and the pH value was fixed at 8.0 ± 0.2. Traces of zinc oxide are detected by PXRD. Chemical analysis gives a Zn^{2+}/Al^{3+} ratio in the LDH near 4.23. A hydration state of 3.9 H_2O molecules/Al^{3+} cation was measured by TGA.

The experimental device (total volume = 40 mL) used for the coprecipitation of porphyrins containing LDHs was adapted to the preparation of small quantities of materials.

$[Zn_3-Al-oTCPP]_{cop}$ is prepared following the same coprecipitation method. The mixed metallic salt solution (0.7 mL of 0.125 M $AlCl_3$ and 0.375 M $ZnCl_2$) and 1 M NaOH solution

(29) Longo, F. R.; Finarelli, M. G.; Kim, J. B. *J. Heterocycl. Chem.* **1969**, *6*, 927.
(30) Srivastava, T. S.; Tsutsui, M. *J. Org. Chem.* **1973**, *38*, 2103.
(31) Leondiadis, L.; Momenteau, M. *J. Org. Chem.* **1989**, *54*, 6135.
(32) Lindsey, J. J. *J. Org. Chem.* **1980**, *45*, 5215.
(33) Dimotakis, E. D.; Pinnavaia, T. J. *Inorg. Chem.* **1990**, *29*, 2393.
(34) De Roy, A.; Forano, C.; El Malki, K.; Besse, J. P. *Anionic Clays: Trends in Pillaring Chemistry, Synthesis of Microporous Materials*; Occeli, M. I., Robson, H. E., Eds.; Van Nostrand Reinhold: New York, 1992; Vol 2, p 108.

Table 2. Preparatives Conditions for $[Zn_R-Al-pTCPP]_{cop}$; for Zn^{2+}/Al^{3+} Equal to *R*, *V* mL of a Mixed *x* Zinc Chloride, and *y* Aluminum Chloride Solution Added to a *V′* mL Solution of *z* *p*TCPP

R (Zn^{2+}/Al^{3+})	*V* (mL)	*x* (mol L^{-1})	*y* (mol L^{-1})	*V′* (mL)	*z* (mol L^{-1})
1	1.60	0.10	0.10	15.0	5.2×10^{-3}
2	1.05	0.17	0.08	15.0	3.0×10^{-3}
3	2.00	0.39	0.13	15.0	8.3×10^{-3}
4	0.90	0.40	0.10	15.0	2.8×10^{-3}
5	1.27	0.25	0.05	15.0	2.1×10^{-3}

were added simultaneously by the means respectively of a push-syringe and an automated titrator, monitored by a pH controller (pH = 7.0 ± 0.2). The flow rate of the solution containing the metal cations was fixed at 2 μL min^{-1}. These reagents are added, under nitrogen atmosphere, to 15 mL of a 2.8×10^{-3} M *o*TCPP solution. This concentration corresponds to twice the number of moles required for the exchange stoichiometry. Reaction and aging were completed after 72 h. The expected amount of anionic porphyrin per Al^{3+} cation in LDH is confirmed by chemical analysis, yielding a Zn^{2+}/Al^{3+} ratio of 2.45.

$[Zn_3-Al-pTSPP]_{cop}$ was synthesized using the same conditions. The reagent solution concentrations are 0.39 M for zinc chloride, 0.13 M for aluminum chloride, 2.7×10^{-3} M for *p*TSPP (1.3 mL), and 1 M for sodium hydroxide.

$[Zn_R-Al-pTCPP]_{cop}$ are synthesized with the same conditions. For Zn^{2+}/Al^{3+} equal to *R*, *V* mL of a mixed *x* M zinc chloride and *y* M aluminum chloride solution is added to a *V′* mL solution of *z* M *p*TCPP and simultaneously to a 1 M sodium hydroxide solution. Values for *R*, *V*, *V′*, *x*, *y*, and *z* are given in Table 2. The chemical analyses of the $[Zn_R-Al-pTCPP]_{cop}$ LDHs are listed in Table 1.

For all these preparations, metal chlorides (Prolabo) and sodium hydroxide (Fluka) were of analytical grade. All of the preparative procedures were performed with deionized water under a nitrogen atmosphere to minimize the competitive intercalation of carbonate anions in LDH arising from adsorption of atmospheric CO_2.

$[Zn_3-Al-pTCPP]_{exc}$ is prepared by anion exchange. *p*TCPP (0.1 g) is dissolved into 25 mL of 0.1 M NaOH. $[Zn_3-Al-Cl]_{cop}$ (0.073 g) is suspended under nitrogen with vigorous stirring in this solution. The exchange is complete after 120 h. The LDH is recovered using the same procedure as for coprecipitation. Chemical analysis is listed in Table 1.

$[Zn_5-Al-pTCPP]_{rec}$ is prepared as follows: $[Zn_5-Al-Cl]_{cop}$ is first calcined at 300 °C for 18 h; the weight loss at this temperature is 21.5%. The calcined product (33 mg) is then dispersed and stirred in 25 mL of a 1.27×10^{-3} M *p*TCPP solution at pH = 8.0 (fixed by the addition of sodium hydroxide) during 24 h. The PXRD pattern shows the presence of a great amount of ZnO. Results of chemical analysis can therefore not be used for the calculation of the LDH chemical composition.

$[Zn_5-Al-pTSPP]_{rec}$ is prepared using the same conditions as above, from 27 mg of calcined $[Zn_5-Al-Cl]_{cop}$ dispersed in 25 mL of a 9.72×10^{-4} M *p*TSPP solution. The recovered product also displays the presence of a large amount of ZnO.

$[Zn_3-Al-pTSPP]_{hyd}$ is obtained by a hydrothermal treatment of $[Zn_3-Al-pTSPP]_{cop}$ under autogeneous pressure, in a stainless steel autoclave fitted with an inner Teflon reactor. $[Zn_3-Al-pTSPP]_{cop}$ (30 mg) is dispersed and stirred (1 h) in 25 mL of deionized water and then heated for 18 h at 120 °C in the autoclave. The product is then recovered by centrifugation and air-dried. The chemical compositions of the LDH phase before and after the hydrothermal treatment is similar.

Instruments. Powder X-ray diffraction patterns of the samples were obtained with a Siemens D501 X-ray powder diffractometer, using Cu Kα radiation and a graphite back monochromator. Diffuse reflectance UV−visible spectra were performed on samples dispersed in Nujol mulls placed in between two quartz slides mounted on the back outlet of an integration sphere (equipped with a SRS-99-010 calibrated diffuse reflectance standard) on a Perkin-Elmer Lambda 2 spectrometer. TGA were recorded on a Setaram TGA 92, at a heating rate of 5 °C/min, under air atmosphere. Chemical analysis of Zn, Al, C, N, H, S were performed in the Vernaison analysis center of CNRS.

Results and Discussion

Synthesis Strategy. Different methods of synthesis are used to prepare layered double hydroxide compounds.[34] Among them, the coprecipitation method, or precipitation at constant pH, allows for the preparation of LDH compounds with a wide variety of divalent and trivalent metals. M^{II} can be Mg, Mn, Fe, Co, Ni, Cu, Zn, and Ca, and M^{III} can be Al, Cr, Mn, Fe, Co, Ga, and La. Other metallic cation associations are encountered, including the monovalent−trivalent combination (Li−Al) or the divalent−tetravalent association (Co−Ti).[34] The $M^{II}-M^{III}$ association in the LDH plays a great role in the structural features and the chemical properties such as the acid−base or the redox properties. Among the various ($M^{II}-M^{III}$) LDH systems, some display a variable composition in M^{II}/M^{III} ratio, while certain phases can be obtained only within a narrow ratio range. Using the coprecipitation preparative route, for example, $[Zn-Al-CO_3]$ LDH can be prepared with a variable Zn/Al ratio in the range 1−3. This property can be advantageously used to tune the layer charge density and then the interlamellar anion concentration. Another interesting feature of this preparative method is that a wide variety of anionic species can be directly intercalated between the hydroxylated sheets. This synthetic route is often the method of choice for the preparation of organic anions containing LDHs which are difficult to obtain in any other ways, and for our purpose, to the synthesis of LDHs intercalated by anionic porphyrins.

The preparation of LDH compounds via anionic exchange reactions on a chloride or nitrate LDH precursor is more straightforward. The efficiency of this route is based on the high expansion properties of the LDH sheets. The interlayer distance values measured for intercalated anionic organic molecules are much higher than that obtained for the largest inorganic anions, i.e., poly(oxometalates). In our case, for instance, the LDH interlayer distance undergoes a large increase from 7.8 to 22.9 Å, during the anionic exchange of Cl^- by $pTCPP^{4-}$. But the exchange is dependent on the nature of the anions to be intercalated; for example, we have observed that organic sulfonates are easily exchanged while carboxylates often display partial or no exchange at all (unpublished results). The strong basic properties of carboxylate groups compared to sulfonate provide them with a great affinity to the hydroxylated layers and probably limits their diffusion in the interlayer domains.

A third preparative route has recently been developed; this is the so-called "reconstruction method".[33−35] It is based on the calcination of a $[M^{II}-M^{III}-CO_3]$ (M^{II}: Mg, Ni, or Zn; M^{III}: Al) LDH precursor at the temperature at which carbonate ions are evolved as CO_2 and metastable amorphous mixed $M^{II}-M^{III}$ oxide compounds are

(35) Chibwe, K.; Jones, W. *J. Chem. Soc., Chem. Commun.* **1989**, 926.

formed. The calcined product is then rehydrated in a solution containing the anion to be intercalated and a new LDH, based on the initial chemical composition of the hydroxylated layer, is reconstructed. The main advantage of this method is the prevention of a competitive intercalation of anions in LDH, and it has been successfully used to prepare pure LDH with alkyl carboxylates or alkyl sulfonates.[35]

We have used these three methods of preparation under optimized conditions, in order to immobilize various amounts of different anionic porphyrins in LDH.

From the chemical analysis results (Table 1), the Zn^{2+}/Al^{3+} ratio in the layers of coprecipitated phases always diverges from the divalent to trivalent ratio in the initial reagent solution. For example, a Zn^{2+}/Al^{3+} of about 2.5 is obtained in LDH from an *R* value of 3.0. This difference can be explained by the uncompleted precipitation of Zn^{2+} at the relatively low coprecipitation pH values that are used to prevent carbonate intercalation. The layer metallic composition has been demonstrated to be strongly dependent on the coprecipitation pH.[36] The higher the Zn^{2+}/Al^{3+} ratio desired in the LDH, the higher coprecipitation pH needed. Table 1 also shows that porphyrins are fully intercalated in LDH in the expected amount, except for *p*TSPP LDH in which only 57% of the total anionic adsorption capacity has been filled. The remaining charge balance is probably filled with chloride and carbonate. The excess amount of carbon often observed is probably due to the high capacity of these basic materials to adsorb CO_2; this is particularly obvious under hydrothermal conditions for $[Zn_3-Al-pTSPP]_{hyd.}$. Coprecipitation and anionic exchange give rise to the same composition of $[Zn_3-Al-pTCPP]$.

When the tetracarboxylate or tetrasulfonate porphyrin is in the free base form the overall charge is 4^- while if it is protonated the charge is reduced to 2^-. For a given layer charge density of the host lattice, the charge compensation by the guest molecules is then insured with twice as much protonated porphyrins than free base porphyrins. The N/Al ratio near to unity confirms that whatever the various preparative conditions used, the different porphyrins are intercalated as the free base form. This result is rather different from the intercalation of porphyrins in Montmorillonites[10] where the acidic properties of the mineral matrix induces protonation of the porphyrins while on the contrary LDH display basic properties.

X-ray Diffraction Study. All of the phases display PXRD diagrams (Figure 2, 3 and 4) typical of LDH. The porphyrin-containing LDHs have a much lower crystallinity than $[Zn_3-Al-Cl]_{cop}$. The diffractograms of the porphyrin LDHs consist of a series of (00*l*) diffraction lines, and a limited number of (*hkl*) lines. These patterns indicate a structural disorganization which probably arises from a turbostratic effect induced by both the highly separated sheets and the weak bonding interactions between the interlayer species and the host lattice.

To improve the crystallinity of the products, we performed various hydrothermal treatments under autogenous pressure. A net increase of the crystallinity was observed only in the case of $[Zn_3-Al-pTSPP]_{cop}$ (treated at 120 °C for 18 h).

A structural study was carried out on the PXR diffractogram of $[Zn_3-Al-pTSPP]_{hyd.}$ the best crystallized phase (Figure 4). It was indexed, like $[Zn_3-Al-Cl]_{cop}$ LDH, in an hexagonal lattice with a 3*R* stacking sequence of the sheets. Values of refined *a* and *c* parameters are listed in Table 3.

A comparison of the PXRD patterns (Figure 2) of the coprecipitated and exchanged [Zn−Al−*p*TCPP] LDHs clearly shows a higher crystallinity for the former

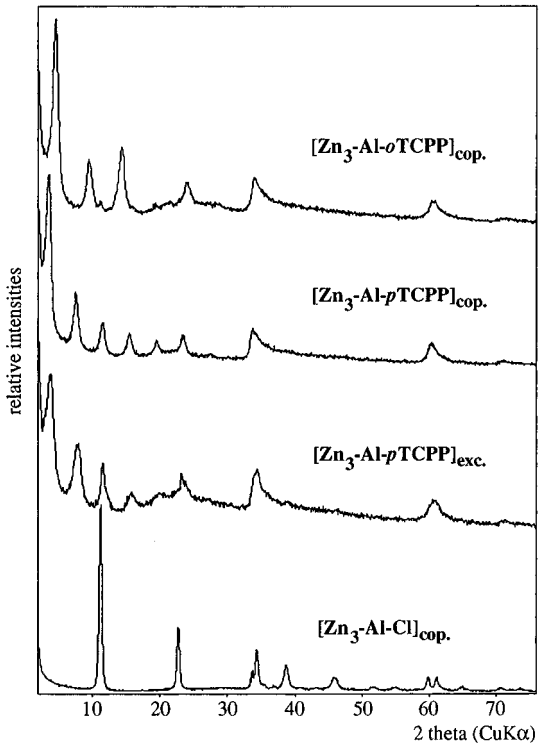

Figure 2. PXRD patterns of $[Zn_3-Al-Cl]_{cop}$, $[Zn_3-Al-pTCPP]_{exc}$, $[Zn_3-Al-pTCPP]_{cop}$, and $Zn_3-Al-oTCPP]_{cop}$.

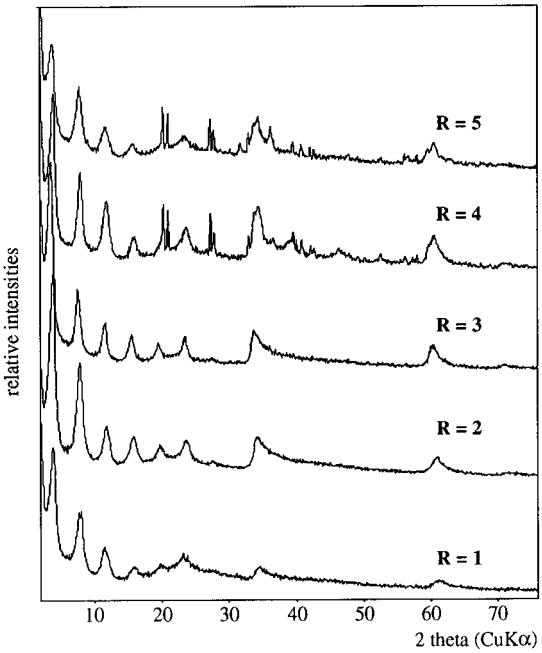

Figure 3. PXRD patterns of $[Zn_R-Al-pTCPP]_{cop}$ with different R = Zn/Al ratio.

(36) Guenane, M.; Forano, C.; Besse, J. P. *Mater. Sci. Forum* **1994**, *152−153*, 343.

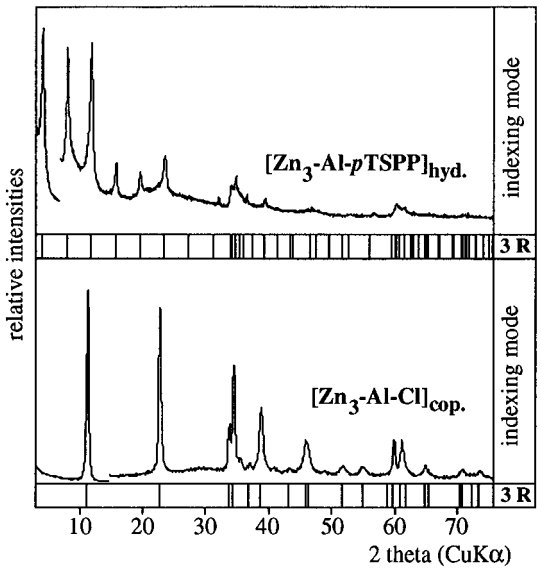

Figure 4. PXRD patterns of $[Zn_3-Al-Cl]_{cop}$ and $[Zn_3-Al-p\text{TSPP}]_{cop}$.

Table 3. PXRD Data of LDH

samples	c (Å)	a or d_{im}[a] (Å)	d_{bs}[b] (Å)
$[Zn_3-Al-Cl]_{cop}$	23.52	3.09	7.84
$[Zn_5-Al-Cl]_{cop}$	23.61	3.10	7.87
$[Zn_1-Al-p\text{TCPP}]_{cop}$	69.27	3.02	23.09
$[Zn_2-Al-p\text{TCPP}]_{cop}$	67.74	3.04	22.58
$[Zn_3-Al-p\text{TCPP}]_{cop}$	68.19	3.06	22.73
$[Zn_4-Al-p\text{TCPP}]_{cop}$	66.72	3.09	22.24
$[Zn_5-Al-p\text{TCPP}]_{cop}$	68.19	3.10	22.73
$[Zn_3-Al-p\text{TCPP}]_{exc}$	68.70	3.05	22.90
$[Zn_3-Al-o\text{TCPP}]_{cop}$	55.62	3.05	18.54
$[Zn_3-Al-p\text{TSPP}]_{cop}$	68.73	3.07	22.91

[a] d_{im} stands for the intermetallic distance. [b] d_{bs} stands for the basal spacing.

compound, as is often observed for highly expanded coprecipitated LDHs.[33]

Figure 3 shows that when varying the initial Zn^{2+}/Al^{3+} ratio (R), pure LDH is obtained only for $R = 2$ and 3. For $R = 4$ and 5, zinc hydroxide (wulfingite) precipitates simultaneously with LDH. For $R = 1$, the large background observed by PXRD around 25° (2θ) is attributed to the presence of a minor aluminum hydroxide amorphous phase. Unfortunately, chemical analysis does not allow us to determine the real Zn^{2+}/Al^{3+} ratio in LDH when other phases precipitate simultaneously. The results indicate that for $R = 1$, 4, and 5 the divalent-to-trivalent metals ratio in LDH diverges from the initial ratio. However, the metallic composition can be estimated from the intermetallic distance d_{im} (equal to twice the d_{110} value); the greater the Al^{3+} amount in LDH, the lower the mean metallic radius and the lower the mean intermetallic distances, d_{im}. Table 3 shows that d_{im} increases linearly up to $R = 3.0$, for the higher values d_{im} differ from the expected values. The domain of the coprecipitated solid solution [Zn−Al−*p*TCPP] seems then to be limited to the upper Zn^{2+}/Al^{3+} value of 3.

The interlayer spacing is known to be also affected by the change in the layer charge density determined by the Zn^{2+}/Al^{3+} ratio. When the charge density increased, the electrostatic interactions between host lattice and interlayer anions increase and a decrease in the basal spacing (d_{bs}) is generally observed. *p*TCPP intercalated LDH presents a basal spacing value between 23.09 and 22.24 Å. As shown in Table 3, the d_{bs} evolution does not follow the expected continuous variation; this is probably due to the effect of different hydration states of the products.[37]

To prepare LDH with higher Zn^{2+}/Al^{3+} ratio, reconstruction of [Zn−Al−*p*TSPP] and [Zn−Al−*p*TCPP] from calcined (300 °C) $[Zn_5-Al-Cl]$ was performed. However, rehydration to an LDH phase was not fully reversible, and the presence of ZnO is always observed which leads to a lower Zn^{2+}/Al^{3+} ratio in the hydroxylated layers than the one expected.

Host and Guest Arrangement. From the LDH d_{bs} values and the dimensions of the anionic macrocycles, it is possible to propose a schematic orientation of the porphyrin between the synthetic mineral sheets. Such a discussion is useful in order to predict the capability of the supported materials to adsorb new guest molecules for catalytic processes electroassisted by metalloporphyrins.

The highest d_{bs} values, 22.7−22.9 Å, are observed for $[Zn_3-Al-p\text{TCPP}]$ and $[Zn_3-Al-p\text{TSPP}]$. The basal spacing can be calculated by the addition of the layer thickness, the dimension of the space occupied by the guest molecules, and the distance between the anions and the layers.

The thickness of the layer is defined as the distance between the two planes of oxygen atoms and has been determined from structural investigations to be 2.0 Å.

The dimensions of the porphyrins are obtained from molecular modeling (Figure 1). The anionic macrocycles have an approximate parallelepiped shape of about 14.6 × 14.6 × 4.3 Å for *p*TSPP, 14.1 × 14.1 × 4.3 Å for *p*TCPP, and 10.9 × 10.9 × 5.7 Å for *o*TCPP.[38]

The observed basal spacings must arise from a perpendicular orientation of the macrocycles to the layers with the four anionic groups interacting with the hydroxylated sheets (Figure 5a). Such a perpendicular arrangement has also been described for other hybrid LDH materials.[3,6,36,39]

This structural model implies hydrogen bonding between the host structure and the guest molecules with distances between the carboxylate and sulfonate anions of the porphyrins and the hydroxyl layers of 3.4 and 3.1 Å, respectively, for *p*TCPP and *p*TSPP LDH. These values are slightly higher than what is usually encountered in carboxylate or sulfonate LDH (2.6−2.7 Å).[36] However, after moderate heating (150 °C), a partial loss of interlayer water molecules reduces the hydrogen bond length to the same value (2.8 Å). This implies further than water molecules take part in the hydrogen-bonding interactions between porphyrins and LDH layers.

The intercalation of the porphyrins in LDH can also be discussed in terms of electrostatic adsorption of the anionic guest molecules onto the surface of the cationic layers. Then adsorption is governed by the charge density of the layers, and the adsorption of the molecules is structurally constrained in order to adapt the

(37) Wang, J.; Tian, Y.; Wang, R. C. Clearfield, A. *Chem. Mater.* **1992**, *4*, 1276.
(38) Stone, A.; Fleisher, E. B. *J. Am. Chem. Soc.* **1968**, *90*, 2735. Coordinate file TPHPORO1 from Cambridge Data Base.
(39) Meyn, M.; Beneke, K.; Lagaly, G. *Inorg. Chem.* **1990**, *29*, 5201.
(40) Gouterman, M. *The Porphyrins*; Dolphin D., Ed.; Academic Press: New York, 1979; Vol. III, Chapter 1.

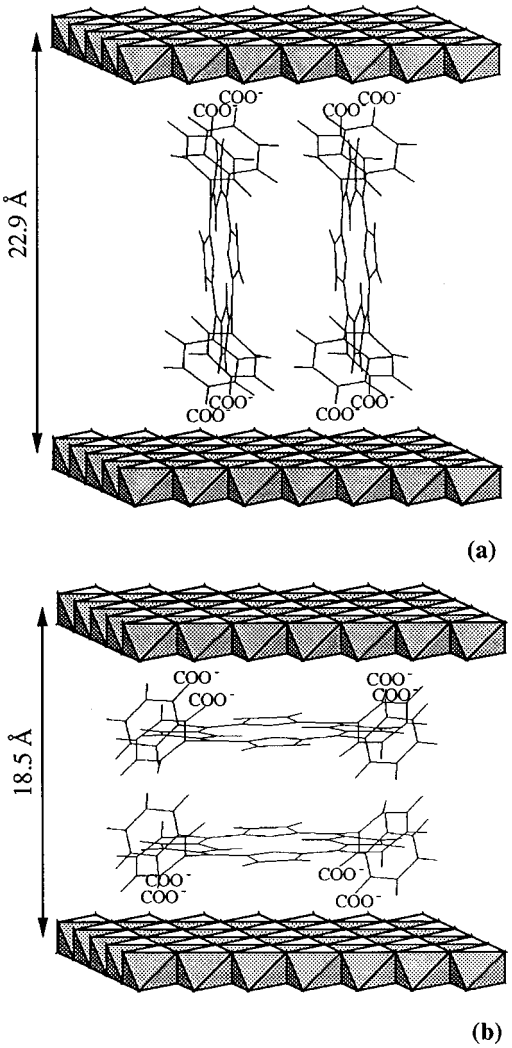

Figure 5. Schematic representation of the *p*TCPP^{4-} (a) and *o*TCPP^{4-} (b) oriented in the interlayers of LDH.

developed surface area per unit charge of the adsorbed molecule to the available surface area per unit charge of the layer. A [Zn−Al] LDH with a theoretical Zn^{2+}/Al^{3+} ratio of 3 displays 33 Å^2 available surface area per unit charge, while the *p*TCPP develops per unit charge two different size edges one of 49 Å^2 and the other of 15 Å^2. Then an orientation of the macrocycle planes parallel to the LDH layers cannot fit with the surface properties of the layers. In a perpendicular orientation to the layer the host lattice offers enough surface (33 Å^2) compared to the small one (15 Å^2) required by the porphyrins. A tilted orientation, which could be envisaged in terms of surface compatibility, would not lead to a satisfactory basal spacing value. Figure 6 presents the projection of the *p*-porphyrins, adsorbed perpendicular to the layer, in the $(\vec{a},\vec{b})$ plane. The arrangement is proposed with the ideal packing. These results allow us to present these LDH as layered compounds pillared by functionalized porphyrins, leaving small cavities of about 7.5 Å diameter.

Phthalocyanines functionalized in para intercalated in LDH have been studied by Carrado et al.[6] and Ukrainczyk et al.[3] A perpendicular arrangement of macrocycles between the layers has been postulated. In a very different manner, the cationic clay minerals intercalate ammonium porphyrins in a flat orientation in hectorite[3,6] or in a slightly tilted position in

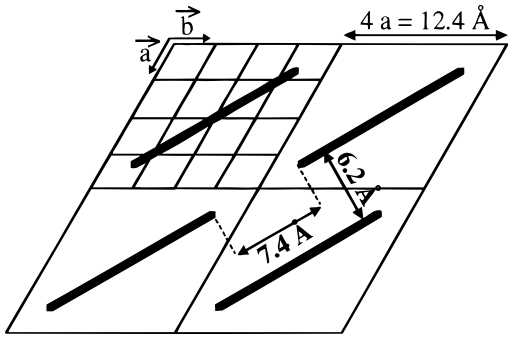

Figure 6. Schematic arrangement of intracrystalline *p*TCPP and *p*TSPP. Projection in the $(\vec{a},\vec{b})$ plane.

montmorillonite.[10,12] This horizontal arrangement is due to the low charge density of these mineral supports and probably stabilized by van der Waals interactions between the silicate layers and the aromatic macrocycles.

In the case of the $[Zn_3-Al-o\text{TCPP}]_{cop.}$, the experimental interlayer spacing (18.5 Å) is lower by about 4 Å than that of the *p*-porphyrin containing LDH. The size of the ortho isomer is 3.2 Å lower than the size of the para isomer. This could fit with a perpendicular orientation of the *o*TCPP, but due to the square-planar arrangement of the four charged groups, which are only on one porphyrin face, such a disposition of the carboxylate groups would prevent the hydrogen-bonding interactions described earlier. Moreover, the difference in the relative intensity ratio between the (006) and (009) diffraction lines, I_{006}/I_{009} for $[Zn_3-Al-p\text{TCPP}]_{cop}$ (I_{006}/I_{009} = 1.61) and $[Zn_3-Al-o\text{TCPP}]_{cop}$ (I_{006}/I_{009} = 0.85), arises from a fundamental change in the organization of the interlayer domains. A planar porphyrin bilayer assembly based on the intercalation of macrocycle with the tetracarboxylate groups pointing away from the medium plane would be more favorable and could also justify the experimental d_{bs} value and the intensity change (Figure 5b). Further, the *o*-porphyrin has a surface per unit charge of nearly (10.9 × 10.9)/4 = 30 Å. The available layer surface area per unit charge is 33 Å^2 on the LDH. These values are compatible with the proposed orientation.

Such an arrangement of the host LDH and the guest ortho-substituted porphyrins has already been suggested for the intercalation of tetrakis(aminophenyl) intercalated into zirconium hydrogen phosphate. This hypothesis was made assuming favorable hydrogen bonding between anions and host phosphonate, along with a good combination of the high density of amine−phosphate interactions due to the plane geometry of charges in this porphyrin.[17] Concerning the LDH intercalated by *o*-α,α,α,α-TCPP, the proposed flat arrangement as dimeric species is based on the trend to dimerize of the porphyrin. A similar bilayer arrangement has already been suggested by Kim and coworkers[17] for *o*-α,α,α,α-tetrakis(aminophenyl)-substituted porphyrins in zirconium hydrogen phosphate.

UV−Visible Absorption Spectra. Absorption bands in the UV−visible region occur in two sets for porphyrins.[40] The Soret band is characterized by a large absorption coefficient and lies in the 400−450 nm range. A second set of weaker bands (the Q bands) occurs between 450 and 700 nm. The free base has four weak

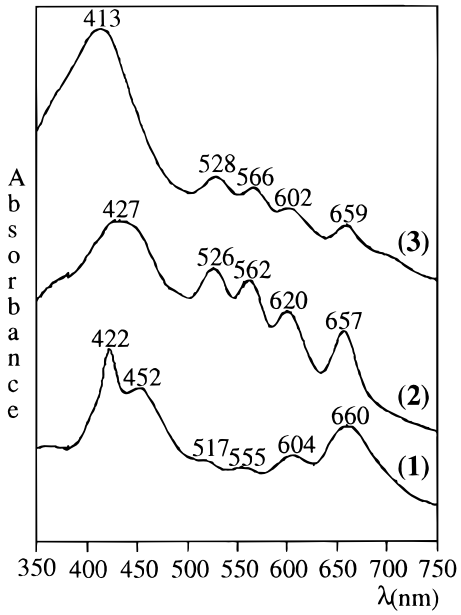

Figure 7. UV−visible spectra of *o*TCPP (1), *p*TCPP (2), and *p*TSPP (3) performed in Nujol mull with an integrating sphere.

Q bands, but protonation to the dication decreases this number to two and also causes the Soret band to shift to higher wavelengths. When the porphyrin is metalated, the UV−visible absorption spectrum contains a Soret band slightly red-shifted from the free base and the Q bands region is strongly modified; only two Q bands are observed between 500 and 650 nm.

UV−visible absorption data for the pure porphyrins and LDH supported porphyrins are illustrated in Figures 7 and 8, respectively. The spectrum of the pure *o*TCPP compound (Figure 7) presents two maxima in the Soret range 422−452 nm and a change in the usual intensity range in the Q bands region since the highest intensities are at 604 and 660 nm. This may be explained by the presence of both free-base and protonated porphyrinic species. A similar spectrum is observed for the *p*TCPP, where the very large Soret band may account for the overlapping of two bands. The *p*TSPP spectrum indicates that no protonated species is observed.

UV−visible absorption data for the different LDH products are illustrated in Figure 8. In the spectrum of [Zn−Al−*o*TCPP]$_{cop}$, the Soret band of *o*TCPPH$_2^{2+}$ has disappeared due to the pH synthesis conditions (pH = 7.0). The Soret band here appears as a thin single peak (434 nm) with a low-wavelength shoulder (424 nm), the higher value accounting probably for the intercalated species. For the Q-band region, the intercalation leads to a general appearance characteristic of free porphyrin. No significant shifts are noted after intercalation. For the [Zn−Al−*p*TCPP], and more particularly for the coprecipitated phase, we note a decrease of the intensity of the two external Q bands usually typical of the metalation of the tetrapyrrole cycle. However according to the chemical analysis such metalation might not exceed 4%. The [Zn−Al−*p*TSPP] spectrum is very similar to the exchanged *p*TCPP LDH phase.

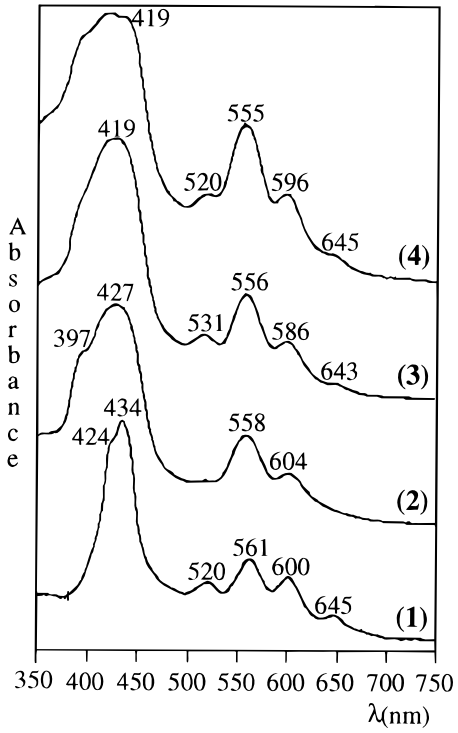

Figure 8. UV−visible spectra of [Zn$_3$−Al−*o*TCPP]$_{cop}$ (1), [Zn$_3$−Al−*p*TCPP]$_{cop}$ (2), [Zn$_3$−Al−*p*TCPP]$_{exc}$ (3), and [Zn$_3$−Al−*p*TSPP]$_{cop}$ (4) performed in Nujol mull with an integrating sphere.

Conclusions

Both coprecipitation at constant pH and anion-exchange methods can be used to prepare anionic porphyrins containing LDH. In terms of the percentage of intercalation, good results are obtained in both cases, but slightly better crystallized materials are prepared with the former method. Selective orientation of the porphyrins between the layers is obtained with para- and ortho-substituted porphyrins. It appears that the interlayer arrangement is determined by both the layer charge density of the host matrix and the isomeric position of the anionic groups substituted on the guest molecules. The perpendicular arrangement of the para carboxylate or sulfonate tetraphenylporphyrinic guest molecules in the LDH interlayer domains is a great advantage compared to their flat orientation on some clays mineral supports for regioselective heterogeneous catalytic reactions. Metalation in situ studies of intercalated free-base porphyrin are now in progress. These new nanocomposite materials are also under investigation as LDH-modified electrodes for electrochemical applications. The ability of porphyrins to penetrate into and to remain bonded to the LDH layers, even under thermal treatment up to 300 °C, encourages us to use such mineral supports for mimetic oxidation reactions of cytochrome P-450.

CM960020T